Visible PL phenomenon at room temperature in disordered structure of SrWO₄ powder

M. ANICETE-SANTOS[a], R.C. LIMA[a], E. ORHAN[b], M.A.M.A MAURERA[c], L.G.P. SIMÕES[a], G. SOUZA[c], P.S. PIZANI[d], E.R. LEITE[a], J.A. VARELA[e] and E. LONGO[e,*]

[a]*Departamento de Química, Universidade Federal de São Carlos, 13565-905 São Carlos, SP, Brazil*
[b]*SPCTS, Université de Limoges, 87000 Limoges, France*
[c]*CCEN Departamento de Química, Universidade Federal da Paraíba, Campus I, 58059-900 João Pessoa, PB, Brazil*
[d]*Departamento de Física, Universidade Federal de São Carlos, 13565-905 São Carlos, SP, Brazil*
[e]*Instituto de Química, Universidade Estadual Paulista, 14801-907 Araraquara, SP, Brazil*

Abstract. The SrWO₄ (SWO) powders were synthesized by the polymeric precursor method and annealed at different temperatures. The SWO structure was obtained by X-ray diffraction and the corresponding photoluminescence (PL) spectra was measured. The PL results reveal that the structural order–disorder degree in the SWO lattice influences in the PL emission intensity. Only the structurally order–disordered samples present broad and intense PL band in the visible range. To understand the origin of this phenomenon, we performed quantum-mechanical calculations with crystalline and order–disordered SWO periodic models. Their electronic structures were analyzed in terms of band structure. The appearance of localized levels in the band gap of the order–disordered structure was evidenced and is a favorable condition for the intense PL to occur.

1. Introduction

CaWO₄ and PbWO₄ are the leading compounds of a family well-known for its photoluminescent properties, the ABO₄ scheelite phases (where A=Ca, Pb, Sr, Ba and B=W, Mo). Their relatively simple crystallographic structures have contributed significantly towards understanding of the photoluminescent property. The scheelite structure is a low density structure enhancing the presence of defects that have profound influence on the static and dynamic properties of these materials.

Although numerous investigations have been realized on the photoluminescent property of scheelite tungstate crystals, there are still issues in debate regarding the origin of the color centers to photoluminescence (PL) emission band, mainly to the centers of green contribution of the band. Groenink and Blasse [1], Lecoq et al. [2], Korzhik et al. [3], and Annenkov et al. [4] concluded that the green emission originates from $(WO_3 + F)$ center in PbWO₄ single crystals. Sokolenko et al. [5] attributed green–red emission to $WO_3 \cdot V\ddot{o}$ oxygen-deficient complexes, Sinelnikov et al. [6]

---

*To whom correspondence should be addressed.

suggested that the WO_4 tetrahedra distorted upon the formation of oxygen vacancies are responsible for the green luminescence band. On other hand, several authors have attributed the PL green component to defect centers with interstitial oxygen: Shi et al. [7], Qi et al. [8], and Chen et al. [9] suggested the ($WO_4 + O_i$) center (where O_i is an interstitial oxygen) as green luminescence center while Huang et al. [10] concluded that the interstitial oxygen O_i enhances the green luminescence.

Barium and strontium tungstate crystals are perspective materials for application of Raman converters, lasers and amplifiers [11–16]. In particular, strontium tungstate is used in solid-state laser systems [17] and recently demonstrated to be a promising nonlinear material for crystalline nano- and picosecond Raman lasers [18].

Orhan et al. [19–22], Longo et al. [23], and Anicete-Santos et al. [24] performed experimental and theoretical studies of the PL property in materials such as perovskite-like titanates and sheelite tungstates. The authors developed ab initio periodic models representing crystalline and order–disordered structures of $Pb(Zr_{0.2}Ti_{0.8})O_3$, $BaTiO_3$, $Ba_{0.5}Sr_{0.5}TiO_3$, and $SrWO_4$. They attributed that the PL high intensity is related to localized states in band gap of order–disordered materials. Table 1 presents the PL results obtained for these materials.

In the present paper, we are combining laboratory experiments and theoretical calculations to understand the PL property in SWO powders. The experimental results present broad and intense PL at room temperature in structurally order–disordered SWO prepared by the polymeric precursor method. To investigate the electronic structure of SWO periodic models representing the crystalline and order–disordered structures were used to give an interpretation in terms of band structure of the conditions allowing PL to occur at room temperature. The aim of our synergetic strategy between experimental and theoretical results is not to explain all the possible PL mechanisms that occur during the photon excitation and decay processes, as many valid hypotheses are already present in the literature, but to discuss the favorable conditions to generate intense PL emission in SWO powders that present structural order–disorder degrees.

2. Experimental

Citric acid ($C_6H_8O_7$) 99.5% purity (Merck), tungstic acid (H_2WO_4) 98% purity (Vetec), strontium carbonate ($SrCO_3$) 99.99% purity (Alfa Aesar), and ethylene glycol

Table 1. PL effect observed in titanates and tungstate

Material	Structure	PL effect	References
$Pb(Zr_{0.2}Ti_{0.8})O_3$ powders	Crystalline	No is observed	20
	Order–disordered	High intensity	
$BaTiO_3$ powders	Crystalline	No is observed	21
	Order–disordered	High intensity	
$Ba_{0.5}Sr_{0.5}TiO_3$ thin films	Crystalline	No is observed	23
	Order–disordered	High intensity	
$SrWO_4$ thin films	Crystalline	Very low intensity	19
	Order–disordered	High intensity	

($C_2H_6O_2$) 99% purity (J. T. Baker) were used as starting materials. Tungsten citrate was formed by the dissolution of tungstic acid in aqueous solution of citric acid under constant agitation. The citrate solution was well stirred and heated at 60 °C to yield a clear and homogeneous solution. Then a $SrCO_3$ salt was added in stoichiometric quantity in the citrate solution. Nitric acid was used to adjust the pH of the solution to 2–3 and to dissolve the salt completely. To promote citrate polymerization, by the polyesterification reaction, ethylene glycol was added with 60:40 proportions (in mass) of citric acid/ethylene glycol. With continuous heating at 60–90 °C, the solution became more viscous but free of any visible phase separation. This solution was then first heat treated at 200 °C during 60 min to pyrolyse the organic material. To remove part of organic material the powder was de-agglomerated and carried at 300 °C for 2 h. The obtained powder was then heat treated in oven from 300 to 700 °C in air for 4 h. This polymeric precursor synthesis method is one of the numerous sol-gel routes commonly used and the advantages that it offers over other synthesis techniques are: low cost, good compositional homogeneity, high purity, and low processing temperatures [25, 26]. The SWO powder was structurally characterized by X-ray diffraction (XRD) using CuKα radiation source with diffraction angle (2θ) ranging between 5 and 75 °C. The diffraction patterns were recorded on a Siemens D5000 machine using a graphite monochromator. The PL spectra of the SWO powders were recorded with a U1000 Jobin–Yvon double monochromator coupled to a cooled GaAs photomultiplier and a conventional photon counting system. The 488 nm exciting wavelength of an argon ion laser was used, with the laser's maximum output power kept at 200 mW. All measurements were taken at room temperature.

3. Computational methods

Calculations were carried out with the Crystal 98 [27] package at the DFT level. The gradient-corrected correlation functional by Lee et al. was used, combined with the Becke3 exchange functional, B3LYP [28, 29] that was demonstrated by Muscat et al. [30] to be suitable to calculate structural parameters and band structures for a wide variety of solid state compounds. The basis sets used to descrive O (6–31G*) and Sr (HAYWSC-31(3d) G) atomic centers can be found at reference [31] and for W in the paper by Cora et al. [32]. The k-points sampling was chosen to be 40 points within the irreducible part of the Brillouin zone. The program OPTIM [33] was used to optimize the cell parameters and atomic positions. The OPTIM is a general optimization tool that minimizes a general function that in this case is the CRYSTAL98-computed total energy. The optimization was realized from experimental data.

The XCrysDen [34] program was used as a graphical tool to design the density of states and the band structure diagrams.

4. Crystal structure and periodic models

The scheelite SWO crystallizes in a tetragonal structure (space group I4$_1$/a, C_{4h}^6 symmetry). Tungsten atoms are surrounded by four oxygen atoms in a tetrahedral configuration and strontium atoms are surrounded by eight oxygens in a pseudo cubic configuration. The experimental cell parameters values [35] are $\mathbf{a} = 5.4136$ and $\mathbf{c} = 11.942$ Å, and the optimized cell parameters are $\mathbf{a} = 5.38250$ and $\mathbf{c} = 11.84602$ Å. The fractional

atomic positions of Sr and W are (0, 1/4, and 5/8) and (0, 1/4, and 1/8), respectively. The experimental values fractional atomic positions of the oxygen in the literature [36] are $x = 0.25(2)$, $y = 0.14(2)$, and $z = 0.075(2)$. The optimized values x, y, and z fractional atomic positions of the oxygen are 0.23244, 0.11121, and 0.04403, respectively.

For computational simplification, the CRYSTAL98 code works in the primitive unit cell rather than in the conventional one. In this case, the primitive cell refined parameters are $a = b = c = 7.04044$ Å, $\alpha = \beta = 135.0530°$, and $\gamma = 65.4479°$. We have used a $1 \times 1 \times 2$ supercell of the primitive cell as a periodic model to represent the crystalline SWO (SWO-c). It results in 24 atoms in the supercell (see Figure 1(a)).

Our aim is to compare the electronic structure of a model standing for the crystalline material to a model representing the powder before crystallization, even if no structural information is available. We know from earlier studies on titanate compounds that during the crystallization process, the network former clusters are the first to be built, as TiO_6 or TiO_5 clusters [37, 38]. From this information and mostly from refs. [1–6, 8, 9] that presume the existence of WO_3 (or highly distorted WO_4) and WO_4 clusters in the scheelite phases, we assume that before the complete crystallization of the powder, i.e. before the heat treatment reaches 700 °C, the structure is composed of a random mixture of WO_4 and WO_3 tetrahedra linked by the Sr ions. We thus created a $1 \times 1 \times 2$ supercell that for the non-crystalline phase based on these assumptions. Starting from the previous SWO-c crystalline model, the W2 and W4 atoms were displaced 0.5 Å in the direction opposite to the starred oxygen atoms of Figure 1(b), in order to break the bonds. This new periodic model will be called SWO-a, representing SWO with a structural order–disorder degree. W2 and W4 atoms are now surrounded by three oxygen atoms in their first coordination sphere.

5. Results and discussion

Figure 2 shows the X-ray diffraction patterns of SWO powders annealed from 300 to 700 °C during 4 h. At 300 °C the material is highly disordered. From 400 °C, the
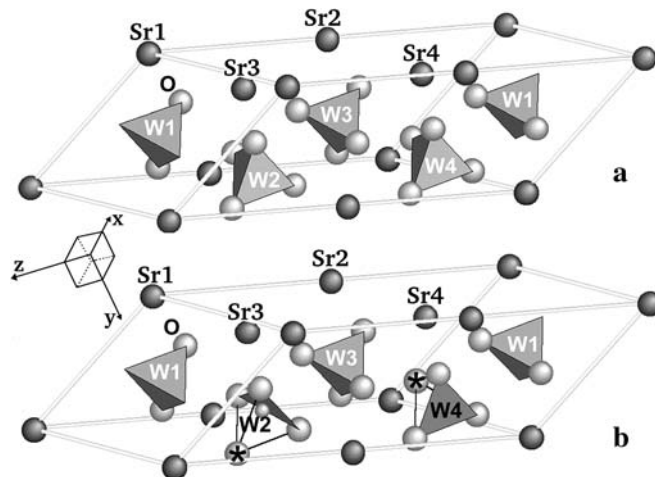

Figure 1. (a) SWO-c periodic model: $1 \times 1 \times 2$ supercell of the SrWO$_4$ primitive unit cell. (b) SWO-a periodic model. W2 and W4 have been shifted by 0.5 Å in the direction opposite to the starred oxygen atoms.
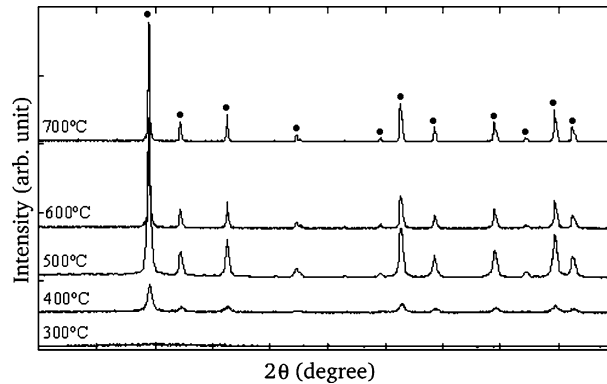
Figure 2. DRX patterns for the SrWO$_4$ powders heat treated from 300 to 700 °C.
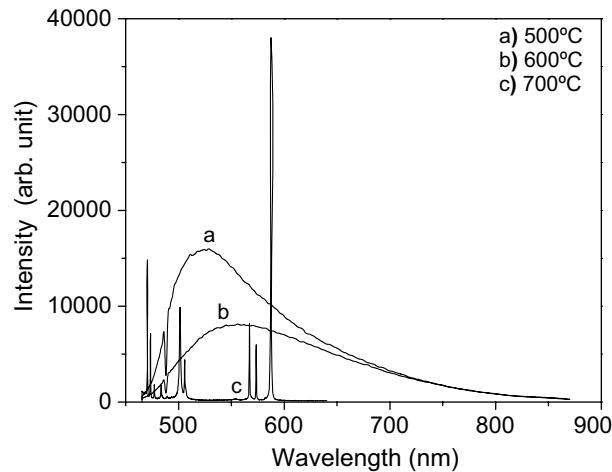

Figure 3. Photoluminescence spectra for the SrWO$_4$ powders heat treated at 500, 600, and 700 °C.

SWO scheelite phase starts to crystallize, without intermediary phase. At 700 °C all the peaks attributed to the scheelite phase are well-defined, showing the complete crystallization of the phase.

The PL spectra recorded at room temperature, for the SWO powders treated at 500, 600, and 700 °C in air atmosphere are shown in Figure 3. The emission takes place in the visible range of the electromagnetic spectra. The bands are broad and intense, mostly for the order-disordered powder annealed at 500 °C. These broad bands are typical of a multiphonon process, i.e. a system in which relaxation occurs by various paths, involving the participation of numerous states. The intensity of the PL emission decreases for the powder annealed at 600 °C. When the SWO powder completely crystallizes, at 700 °C, no PL is observed, only the Raman modes are observed. Therefore, the PL intensity is linked to the thermal treatment history of the material and consequently to the structural order–disorder degree in the lattice. To understand the origin of visible PL at room temperature in order–disordered SWO, we performed quantum-mechanical calculations of periodic models.
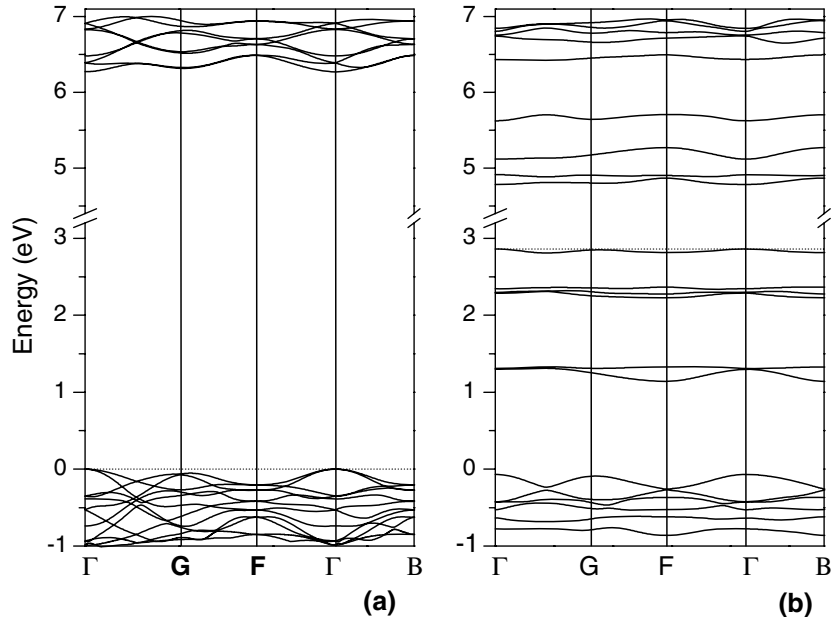
Figure 4. (a) Band structure for the SWO-*c* model. (b) Band structure for the SWO-*a* model. The zero corresponds to the Fermi energy of the SWO-*c* model to facilitate comparison.

In Figure 4(a) the calculated band structure of bulk SWO-*c* model is plotted along four symmetry directions in the first Brillouin zone. The SWO-*c* model can be designed as $(WO_4)–(WO_4)$, as each tungsten is surrounded by four oxygen in a C_{4h}^6 configuration, and the SWO-*a* model can be designed as $(WO_4)–(WO_3)$. With these two models, we can compare the electronic structure of the crystalline and order–disordered structures. In the SWO-*a* model, each of the (WO_4) is accompanied by a (WO_3) cluster formed by the distortion induced by the atom displacements. The resulting disorder will lead to sizeable local potential fluctuations to which each (WO_3) and (WO_4) contributes, as well as adjusts itself in a self-consistent way.

Our aim with the use of this SWO-*a* model is to offer a simple scheme allowing to understand the effects of structural deformation on the electronic structure without completely suppressing the geometry of the cell that is useful for the periodic calculations. Using the same kind of distorted model we have successfully explained the PL of various perovskite titanates [23, 39, 40]. The SWO-*c* model presents a direct band gap of 6.27 eV at the Γ point. In Figure 4(b) in the asymmetric SWO-*a* model localized levels in the band gap appear and they are linked to the defects in the lattice. SWO-*a* model also presents a direct band gap at Γ point and its value is 1.92 eV.

In Figure 5, the contributions of the dominant orbitals for each band at the Γ point are schematically represented as energy levels for both periodic models. A square modulus coefficient of 0.25 was chosen to select the contributions of the orbitals greater than 0.25 weight value. For SWO-*c* model (Figure 5(a)) the highest occupied crystal orbital (HOCO) is degenerated and its dominant character is $2px$ and $2py$ of the 16 oxygens of the supercell. The lowest unoccupied crystal orbital (LUCO) is predominantly made of the $5dz^2$ levels of the four tungsten atoms. Although the WO_4 tetrahedra is regular, the $5d$ orbitals splitting is not the
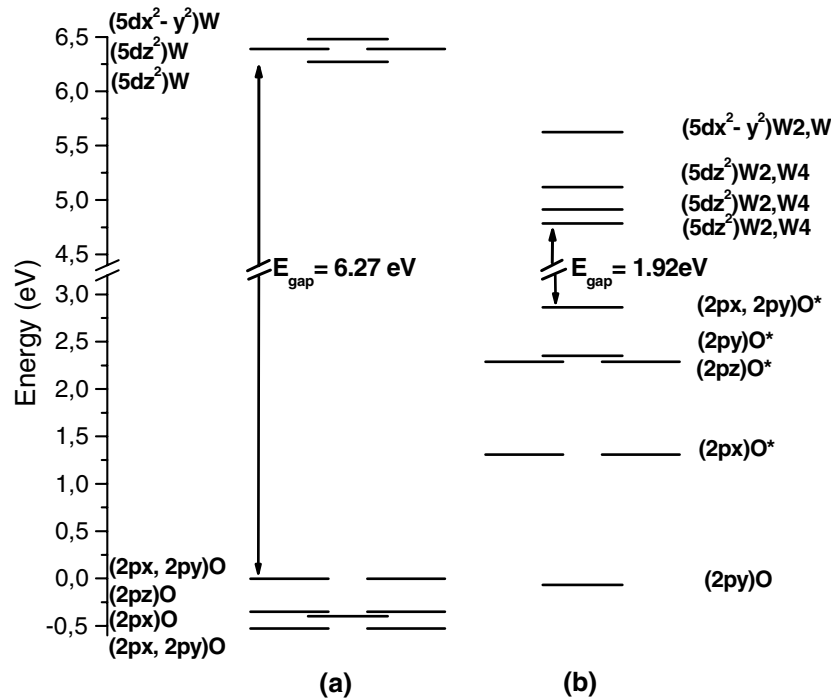
Figure 5. Representation of the main atomic orbitals contributions to the crystal orbitals taken at Γ point for SWO-*c* (a) and SWO-*a* (b).

classical e − t₂ splitting because the tetrahedra do not have the same orientation (see Figure 1). In Figure 5(b), which illustrates the orbital levels for SWO-*a* model, the HOCO and LUCO are not degenerated owing to the fact that there has been a loss of symmetry. $5dz^2$ remains the main character of LUCO and the HOCO is still made of $2p$ levels, but mainly of the O* atomic levels, the two oxygen atoms that lost connection with W2 and W4 tungsten atoms, see Figure 1(b). All the localized levels that appear above the valence band of SWO-*c* are of mainly O* character. The $5d$ character of W2 and W4 atoms also form localized levels below the conduction band.

The hypothesis that we have proposed throughout our studies concerning the origin of PL at room temperature in structurally order–disordered tungstates must fulfill two conditions: (i) to possess two types of differently charged clusters creating a polarization in the structure, as (WO₄)–(WO₃) and (ii) to present some localized levels inside its band gap (Figure 5(b)), levels that result mostly from structural disorder. The junction of those two conditions allow an easy trapping of electrons and holes during photon excitations and thus favors the radiative decay causing PL emission. In order–disordered SWO these two conditions are found and this is the reason of the strong PL observed.

6. Conclusions

The SWO powders have been synthesized following a soft chemical processing and visible PL has been evidenced. They were structurally characterized by means of X-ray diffraction. PL measurements indicated that the behavior of intense and broad

PL at room temperature must be related to the structural order–disorder of the material.

By first principles calculations, a detailed analysis of electronic structure reveals that the main character of the localized levels above the valence band are of $2p$ levels of the oxygen atoms, that lost connection with the W2 and W4 tungsten atoms. The levels that appear below the conduction band are mainly of character $5dz^2$ of these tungsten atoms.

These results show that the chosen theoretical models are in good agreement with the experimental data and with the interpretation that the photoluminescence and the band gap are controlled by structural order–disorder in the SWO lattice.

Acknowledgements

References

1. Groenink, J.A. and Blasse, G., J. Solid State Chem., 32 (1980) 9.
2. Lecoq, P., Dafinei, I., Auffray, E., Schneegans, M., Korzhik, M.V., Missevitch, O.V., Pavlenko, V.B., Fedorov, A.A., Annenkov, A.N., Kostylev, V.L. and Ligun, V.D., Nucl. Instrum. Meth. A, 365 (1995) 291.
3. Korzhik, M.V., Pavlenko, V.B., Timoschenko, T.N., Katchanov, V.A., Singovskii, A.V., Annenkov, A.N., Ligun, V.A., Solskii, I.M. and Peigneux, J.P., Phys. Status Solidi A, 154 (1996) 779.
4. Annenkov, A.A., Korzhik, M.V. and Lecoq, P., Nucl. Instrum. Method. A, 490 (2002) 30.
5. Sokolenko, E.V., Zhukovskii, V.M., Buyanova, E.S. and Krasnobaev, Y.A., Inorg. Mater., 34 (1998) 499.
6. Sinelnikov, B.M., Sokolenko, E.V. and Zvekov, V.Y., Inorg. Mater., 32 (1996) 999.
7. Shi, C., Wei, Y., Yang, X., Zhou, D., Guo, C., Liao, J. and Tang, H., Chem. Phys. Lett., 328 (2000) 1.
8. Qi, Z., Shi, C., Zhou, D., Tang, H., Liu, T. and Hu, T., Physica B, 307 (2001) 45.
9. Chen, Y., Shi, C. and Hu, G., J. Appl. Phys., 87 (2000) 1503.
10. Huang, Y., Zhu, W. and Feng, X., J. Electron Spectrosc. Relat. Phenom., 133 (2003) 39.
11. Zverev, P.G., Basiev, T.T., Sobol, A.A., Skornyakov, V.V., Ivleva, L.I., Polozkov, N.M. and Osiko, V.V., Quantum Electron., 30 (2000) 55.
12. Basiev, T.T., Sobol, A.A., Zverev, P.G., Osiko, V.V. and Powell, R.C., Appl. Optics, 38 (1999) 594.
13. Basiev, T.T., Sobol, A.A., Voronko, Y.K. and Zverev, P.G., Opt. Mater., 15 (2000) 205.
14. Zverev, P.G., Basiev, T.T., Osiko, V.V., Kulkov, A.M., Voitsekhovskii, V.N. and Yakobson, V.E., Opt. Mater., 11 (1999) 315.
15. Basiev, T.T., Sobol, A.A., Zverev, P.G., Ivleva, L.I., Osiko, V.V. and Powell, R.C., Opt. Mater., 11 (1999) 307.
16. Cerny, P., Jelinkova, H., Zverev, P.G., and Basiev, T.T., Prog. Quantum Electron., 28 (2004) 113.
17. Grasser, R., Pompe, W. and Scharmann, A., J. Lumin., 40–41 (1988) 343.
18. Voronina, I.S., Ivleva, L.I., Basiev, T.T., Zverev, P.G. and Polozkov, N.M., J. Opt. Adv. Mat., 5 (2003) 887.
19. Orhan, E., Anicete-Santos, M., Maurera, M.A.M.A., Pontes, F.M., Paiva-Santos, C.O., Souza, A.G., Varela, J.A., Pizani, P.S. and Longo, E., Chem. Phys., 312 (2005) 1.
20. Orhan, E., Pontes, F.M., Leite, E.R., Pizani, P.S., Varela, J.A. and Longo, E., Chem Phys Chem, 6 (2005) 1530.

21. Orhan, E., Varela, J.A., Zenatti, A., Gurgel, M.F.C., Pontes, F.M., Leite, E.R., Longo, E., Pizani, P.S., Beltràn, A. and Andrès, J., Phys. Rev. B, 71 (2005) 085113.
22. Orhan, E., Anicete-Santos, M., Maurera, M.A.M.A, Pontes, F.M., Souza, A.G., Andrés, J., Beltrán, A., Varela, J.A., Pizani, P.S., Taft, C.A. and Longo, E., J. Solid State Chem., 178 (2005) 1284.
23. Longo, E., Orhan, E., Pontes, F.M., Pinheiro, C.D., Leite, E.R., Varela, J.A., Pizani, P.S., Boschi, T.M., Lanciotti, F. Jr., Beltràn, A. and Andrès, J., Phys. Rev. B, 69 (2004) 125115.
24. Anicete-Santos, M., Cavalcante, L.S., Orhan, E., Paris, E.C., Simões, L.G.P., Joya, M.R., Rosa, I.L.V., de Lucena, P.R., Santos, M.R.M.C., Santos-Júnior, L.S., Pizani, P.S., Leite, E.R., Varela, J.A. and Longo, E., Chem. Phys., 316 (2005) 260.
25. Pontes, F.M., Leite, E.R., Pontes, D.S.L., Longo, E., Santos, E.M.S., Mergulhao, S., Pizani, P.S., Lanciotti, F., Boschi, T.M. and Varela, J.A., J. Appl. Phys., 91 (2002) 5972.
26. Pontes, F.M., Maurera, M.A.M.A., Souza, A.G., Longo, E., Leite, E.R., Magnani, R., Machado, M.A.C., Pizani, P.S. and Varela, J.A., J. Eur. Ceram. Soc., 23 (2003) 3001.
27. Saunders, V.R., Dosevi, R., Roetti, C., Causa, M., Harrison, N.M. and Zicovich-Wilson, C.M., CRYSTAL98 User's Manual, University of Torino, Torino, 1998.
28. Lee, C., Yang, W. and Parr, R.G., Phys. Rev. B, 37 (1988) 785.
29. Becke, A.D., J. Chem. Phys., 98 (1993) 5648.
30. Muscat, J., Wander, A. and Harrison, N.M., Chem. Phys. Lett., 342 (2001) 397.
31. http://www.crystal.unito.it/Basis_Sets/Ptable.html.
32. Cora, F., Patel, A., Harrison, N.M., Dovesi, R. and Catlow, C.R.A., J. Am. Chem. Soc., 118 (1996) 12174.
33. Cabal, V.L., OPTIM User's Manual, Departamento de Quimica Fisica y Analitica, University of Oviedo, Oviedo, Spain (1998).
34. Kokalj, A., J. Mol. Graph., 17 (1999) 176.
35. Sleight, A.W., Acta. Crystall. Section. B-struc. B, 28 (1972) 2899.
36. Gurmen, E., Daniels, E. and King, J.S., J. Chem. Phys., 55 (1971) 1093.
37. Pontes, F.M., Longo, E., Leite, E.R., Lee, E.J.H., Varela, J.A., Pizani, P.S., Campos, C.E.M., Lanciotti, F., Mastellaro, V. and Pinheiro, C.D., Mater. Chem. Phys., 77 (2003) 598.
38. Leite, E.R., Pontes, F.M., Paris, E.C., Paskocimas, C.A., Lee, E.J.H., Longo, E., Pizani, P.S., Varela, J.A. and Mastelaro, V., Adv. Mater. Opt. Electron., 10 (2000) 235.
39. Pontes, F.M., Pinheiro, C.D., Longo, E., Leite, E.R., de Lazaro, S.R., Varela, J.A., Pizani, P.S., Boschi, T.M. and Lanciotti, F., Mater. Chem. Phys., 78 (2003) 227.
40. Orhan, E., Pontes, F.M., Santos, M.A., Leite, E.R., Beltran, A., Andres, J., Boschi, T.M., Pizani, P.S., Varela, J.A., Taft, C.A. and Longo, E., J. Phys. Chem. B, 108 (2004) 9221.